Force spectroscopy reveals the presence of structurally modified dimers in transthyretin amyloid annular oligomers.

Pires RH, Saraiva MJ, Damas AM, Kellermayer MS.

Published in: J Mol Recognit. 2017 Mar;30(3).

doi: 10.1002/jmr.2587.

First published online: 2016 Nov 3.

Accepted in J. Mol. Rec.

Force Spectroscopy Reveals the Presence of Structurally Modified Dimers in Transthyretin Amyloid Annular Oligomers.

Ricardo H. Pires[1,#,*], Maria J. Saraiva[3,4], Ana M. Damas[3,4], and Miklós S. Z. Kellermayer[1,4,*]

[1]Department of Biophysics and Radiation Biology, Semmelweis University, Budapest, Hungary.
[2]Institute for Molecular and Cell Biology (IBMC), Porto, Portugal.
[3]Instituto de Ciências Biomédicas de Abel Salazar (ICBAS), Universidade do Porto, Porto, Portugal.
[4]MTA-SE Molecular Biophysics Research Group, Budapest Hungary
[#]Current Address: ZIK-HIKE, University of Greifswald, Greifswald, Germany

*Correspondence:
RHP: piresr@uni-greifswald.de; MSZK: kellermayer.miklos@med.semmelweis-univ.hu
.

ABSTRACT

Toxicity in amyloidogenic protein misfolding disorders is thought to involve intermediate states of aggregation associated with the formation of amyloid fibrils. Despite their relevance, the heterogeneity and transience of these oligomers have placed great barriers in our understanding of their structural properties. Among amyloid intermediates annular oligomers or annular protofibrils have raised considerable interest because they offer a mechanism of cellular toxicity via membrane permeation.

Here we investigated, by using AFM force spectroscopy, the structural detail of amyloid annular oligomers from transthyretin (TTR), a protein involved in systemic and neurodegenerative amyloidogenic disorders. Manipulation was performed *in situ*, in the absence of molecular handles and using persistence length fit values to select relevant curves. Force curves reveal the presence of dimers in TTR annular oligomers that unfold via a series of structural intermediates. This is in contrast with the manipulation of native TTR, that was more often manipulated over length scales compatible with a TTR monomer and without unfolding intermediates. Imaging and force spectroscopy data suggest that dimers are formed by the assembly of monomers in a head-to-head orientation with a non-native interface along their β-strands. Furthermore, these dimers stack through non-native contacts that may enhance the stability of the misfolded structure.

INTRODUCTION

Amyloid aggregates are among some of the most deleterious and frequent agents of protein folding diseases including disorders with neurological (Alshehri *et al.* 2015), cardiac (Maleszewski 2015, Wechalekar *et al.* 2015) or systemic manifestations (Wechalekar *et al.* 2015). In the typical end stage of amyloidogenesis micrometer-long amyloid fibrils deposit and accumulate in various tissues of the patients (Wechalekar *et al.* 2015). This is the case with transthyretin (TTR), a homotetrameric serum-circulating protein involved in the transport of thyroxin and the co-transport of retinol (Robbins 2002). TTR monomers (Figure 1) contain a single α-helix and two β-sheets, each composed of 4 β-strands (DAGH and CBEF), and display a so-called "β-sandwich" fold that resembles a "flattened β-barrel" with its two β-sheets packed together mostly through hydrophobic interactions of its side chains (Damas *et al.* 2000). A TTR dimer is formed through hydrogen bonding across H-H' and F-F' chains between two TTR monomers, and the final tetrameric arrangement results from two dimers that face each other through the DAGH β-sheet in a twofold symmetric fashion. (Damas *et al.* 2000). The dimer-dimer interface in the equatorial plane of the tetramer delineates the contours of a pair of cavities for thyroxin binding. The binding of thyroxin and other similar small ligand molecules further stabilizes the tetrameric arrangement (Johnson *et al.* 2005).

To some extent the wild-type form of TTR appears to be prone to amyloid aggregation as evidenced by cases of senile systemic amyloidosis where WT TTR is found in amyloid deposits (Nakagawa *et al.* 2016). However, certain mutations in the TTR sequence can greatly enhance the process of aggregation even though no particular amyloidogenic hotspot can be assigned (Nagasaka 2012, Alshehri *et al.* 2015). In spite of this, *in vitro* aggregation of WT TTR and of most of its amyloidogenic variants is often induced by mild acidification (Lai *et al.* 1996), which has been proposed to mimic the lysosomal environment associated with the conversion of proteins and peptides into their amyloidogenic form (Lai *et al.* 1996, Nixon *et al.* 2006, Naiki *et al.* 2016). The resulting aggregates typically bind the amyloid markers Thioflavin-T and Congo red (Cardoso *et al.* 2002, Pires *et al.* 2011), display a high content of β-sheets (Faria *et al.* 2015), but lack the morphology of fibrils extracted from patient samples (Cardoso *et al.* 2002, Annamalai *et al.* 2016).

While partial unfolding of the TTR monomer and disassembly of the tetramer is a prerequisite for fibrillation (Groenning *et al.* 2015, Saelices *et al.* 2015), there is strong debate over the details of the rest of the aggregation pathway. Some studies suggest that *in vitro* fibrillation is driven through the addition of monomers (Quintas *et al.* 1997, Cardoso *et al.* 2002, Groenning *et al.* 2015), while others have highlighted the role of oligomeric species as active participants in the fibrillogenesis

process (Serag *et al.* 2001, Pires *et al.* 2011, Pires *et al.* 2012, Faria *et al.* 2015). Amyloid oligomers from different proteins have been proposed to be off-pathway oligomeric assemblies (Pires *et al.* 2011, Mulaj *et al.* 2014) that share certain structural characteristics with amyloid fibrils, yet do not directly seed the fibrils (Mulaj *et al.* 2014, Yagi *et al.* 2014). Nonetheless, amyloid oligomers are viewed with extreme interest since they are likely to be a main source of amyloid toxicity in vivo (Diomede *et al.* 2014, Harte *et al.* 2015).

While the mechanisms of amyloid toxicity remain unclear for the most part, interference with the cell membrane appears to be required (Cecchi *et al.* 2013, Naiki *et al.* 2016). Amyloid fibrils have been increasingly recognized as a condensed state of misfolded proteins which is less harmful than the amyloid oligomers associated with them (Cecchi *et al.* 2013, Harte *et al.* 2015). Among the different types of amyloid oligomers (Cecchi *et al.* 2013), those with annular morphology, termed either as annular oligomers or annular protofibrils, have received significant attention. They have been described across a variety of amyloid systems, and since toxicity appears to develop through poration of the cell membrane, annular oligomers have emerged as possible candidates behind amyloid toxicity (Mirzabekov *et al.* 1996, Capone *et al.* 2009). However, their transient nature (Pires *et al.* 2012) together with the polymorphism associated with amyloid protein aggregation has placed great barriers towards understanding their molecular structure and properties.

Here we have used AFM-based force spectroscopy to obtain greater insight into the structure of TTR annular oligomers. We observed that they unfold via a series of intermediates which we have characterized in terms of forces associated with contour-length increments. Our data allows us to put forward a structural model for the organization of the TTR monomer within the annular assembly.

MATERIALS AND METHODS

Sample Preparation. Recombinant WT TTR expressed in BL21 *E. coli* was isolated as described previously (Almeida *et al.* 1997) and further purified to high purity by using anion exchange (MonoQ column, GE Healthcare) and size exclusion (Superdex S75 column, GE Healthcare) chromatography steps (Pires *et al.* 2011). Stock solutions of WT TTR of 4-8 mg/mL were kept in 10 mM HEPES, pH 7.0 at −20°C. Protein quantification was performed by spectrophotometry at 280 nm (ε = 77600 M^{-1} cm^{-1}). TTR amyloid aggregation was induced by diluting TTR to a final concentration of 1 mg/mL in 50 mM sodium acetate buffer at pH 3.6 and incubating at 37 °C (Pires *et al.* 2011, Pires *et al.* 2012). Typically, within 24h of incubation transient oligomeric assemblies with annular shape were observed as reported previously (Pires *et al.* 2012).

Atomic Force Microscopy and Force Spectroscopy. Data acquisition was performed in liquid and at room temperature with an MFP-3D Atomic Force Microscope (Asylum Research, Santa Barbara, USA), using a cantilever (Biolever A, Olympus) with a resonance frequency in liquid of ~9.2 kHz. Non-contact (AC) mode AFM images were acquired using free and set-point amplitudes of ~0.3 V and ~0.2 V, respectively. Images of 1024×512 and 512×512 pixels were obtained at a line-scanning frequency of ~0.8 Hz. Typically, 3h prior to probing the sample by AFM, 1×1 cm^2 of V-1 grade muscovite mica surfaces were modified with glutaraldehyde as described earlier (Wang *et al.* 2002). Briefly, 300 µL of aminopropyltriethoxysilane (Sigma), 100 µL N,N-diisopropylethylamine (Sigma), and freshly cleaved mica sheets were sequentially placed inside a sealed desiccator with ~5 L volume, and its atmosphere was purged with argon gas. After 3h of vapour deposition, mica sheets were removed and 200 µL of 1 mM glutaraldehyde (Sigma) wad pipetted onto the modified surface, incubated for 10 min at room temperature, washed extensively with MilliQ water and finally with the sample buffer. Typically, 100 µL of sample was then added on the surface and subsequently washed with sample buffer after 10 min. Immediately before deposition, samples were prepared by diluting stock solutions of WT TTR down to 0.5 µg/ mL in 10 mM HEPES buffer, pH 7 and 150 mM NaCl, while acidified amyloid samples were diluted to 1-3 µg/mL in 50 mM sodium acetate buffer at pH 3.6. The cantilever deflection was calibrated against the surface of freshly cleaved mica, and the spring constant of the cantilever (typically ~30 pN/nm) was determined with the thermal method (Hutter *et al.* 1993). After image acquisition, *in situ* force spectroscopy to promote mechanical unfolding of single molecules was performed by pressing the cantilever tip onto pre-selected coordinates of the image and moving the cantilever away from the surface with a constant, typical velocity of 500 nm/s.

Data Processing and Analysis. All data were processed using Igor Pro 6 and built-in procedures developed by the AFM manufacturer for analysis of data obtained with the instrument. Force-extension curves collected during cantilever retraction (pulling) contained several sawtooth-type force-transitions, the rising halves of which were fitted with the worm-like chain (WLC) model of entropic elasticity:

$$F = \frac{k_B \cdot T}{L_P}\left[\frac{1}{4}\left(1 - \frac{z}{L_C}\right)^{-2} - \frac{1}{4} + \frac{z}{L_C}\right]$$

where F is force, z is extension, T is temperature, k_B is the Boltzmann constant, L_C is the contour length and L_P is the persistence length. The main criterion used to select force curves was the analysis of the persistence length whereby curves containing a majority of events with $L_P < 300$ pm were discarded. Selected curves were again fitted with the WLC model constrained to $L_P = 400$ pm to determine the contour length for each force transition. Statistical significance was determined using the Wilcoxon signed-rank test. Error values indicated in the text are standard errors of the mean (s.e.m.). Relevant statistics are tabulated in the Supplementary information section (Table S1).

RESULTS

Transthyretin amyloid annular oligomers (aoTTR) were observed within the first 24 hours after commencement of aggregation by acidification as reported earlier (Pires *et al.* 2012). Evidence of their annular morphology was apparent in the height-, amplitude- and phase-contrast AFM images (Figure 2A). Height-contrast images show topological properties similar to our previous report (Pires *et al.* 2012), notably a diameter of ~15 nm (Figures 2B and 2C) and heights of 2.47 ± 0.09 nm (Figures 2C and 2E). These characteristics are markedly different from those obtained on native TTR (nTTR), which was imaged in PBS (Figure 2D) showing the presence of globular particles with heights of 1.03 ±0.05 nm (Figure 2E).

Both nTTR and aoTTR were manipulated by force spectroscopy. The obtained force curves showed marked differences in both the extension of the manipulated chains and in the number of intermediates occurring during pulling (Figure 3A). While in the case of nTTR, force curves typically exhibited a single mechanical event corresponding to the detachment of the molecule from the tip, in case of aoTTR we often observed curves containing up to eight events (Figure 3B). The curves were fitted with the WLC model to reveal the parameters of the manipulated protein chain. The persistence length values were distributed around 0.4 nm: mean values were 0.491 ± 0.017 nm and 0.464 ± 0.019 nm for nTTR and aoTTR, respectively (Figure 3C). In subsequent analyses we used 0.4 nm in the WLC fits to obtain the contour lengths (L_C) associated with the protein chains and the intermediate states of mechanical unfolding.

We began by analyzing the *Lc* of the last observed event, or the maximal contour length (Lc-Max) corresponding to the detachment of the sample from the tip. While in the case of nTTR a limit of up to ~50 nm was typically attained, this was often approximately the double in the case of aoTTR (Figure 4A). Considering that the TTR monomer with its N-terminal signal methionine has 128 residues and therefore a contour length (Lc-Monomer) of 51.2 nm, the results may also be expressed as a fraction of the length of the TTR monomer. This analysis shows (Figure 4A) that when manipulating nTTR, typically we stretched, on average, a fractional size of 0.66 ± 0.02 of the TTR monomer. By contrast, for aoTTR the fractional size was on average 1.41 ± 0.03 ($p<0.001$). This is also apparent when examining the *Lc* associated with the subsequent unfolding events as a function of their rank within the sequence of the force spectrum (Figure 4B). The subsequent unfolding events typically occurred separated by approximately 10 nm, and up to ~48 nm for nTTR and up to ~88 nm for aoTTR. The spacing between intermediate events (ΔLc) was analyzed more carefully for aoTTR (Figure 4C). Because the position of the last event is randomly located since it

is determined by the site of tip-sample interaction and the moment of detachment, the spacing between the two last events was excluded from the analysis. The histogram displays a multimodal distribution where peaks appear at multiples of 4 nm and up to 18 nm. Typically, transitions occurred separated by ~8 nm, representing 50% of the analyzed ΔLc values. These intermediate transitions also occurred at increased force for aoTTR when compared with nTTR (Figure 4D), or 95 ± 4 pN and 57 ± 10 pN respectively ($p<0.001$).

DISCUSSION

AFM imaging of amyloid annular oligomers.

Amyloid annular oligomers have been imaged by AFM during aggregation of different proteins (Quist *et al.* 2005, Sbrana *et al.* 2007, Pires *et al.* 2012, Lasagna-Reeves *et al.* 2014). Compared to other annular assemblies such as ion channels (Muller *et al.* 2007), the AFM images of amyloid annular oligomers are often more fuzzy, possibly due to the fact that, on one hand, annular oligomers are unstable complexes and, on the second, because their orientation is likely more random than in the case of membrane proteins. They nonetheless reveal an annular configuration (Figure 2A) that is more striking in the phase-contrast AFM images as seen also earlier (Pires *et al.* 2012). Topographic mapping further indicates that these oligomeric species have morphological properties similar to those previously identified in the TTR aggregation pathway (Pires *et al.* 2012), including diameters in the range of 15 nm (Figures 2B and C) and heights of ~2.5 nm (Figure 2E). By contrast, images of TTR in PBS displays the presence of particles with an average height of ~1 nm. As reported earlier based on volume calculations derived from AFM data, these particles are likely to represent mostly TTR monomers (Pires *et al.* 2012). Although the functional TTR is a tetramer, upon extreme dilutions such as those required for AFM imaging, the TTR tetramer tends to dissociate into its constituting units even at physiological conditions of pH and ionic strength (Quintas *et al.* 1997). However, we can also notice some extent of heterogeneity in the particle population (Figure 2D) which may not be so clear from the height measurements alone (Figure 2F) but becomes more apparent when volume calculations are used (Pires *et al.* 2012). Thus, nTTR samples appear to be composed mostly of TTR monomers and to a smaller extent also of dimers and tetramers.

Persistence length as a selection criterion of force curves.

Manipulation of nTTR and aoTTR resulted in sawtooth-shaped force transitions present at extensions up to ~ 100 nm (Figure 3). These force curves revealed transitions that occurred several times in any one pulling of aoTTR, while in the case of nTTR most often only a single event resulting from sample-tip detachment was observed (Figure 2B). Protein unfolding experiments by SMFS typically involve either the usage of molecular handles through which tension is applied to the system being probed (Cecconi *et al.* 2011, Ott *et al.* 2016) or rely on natural or recombinant systems consisting of a series of concatenated polypeptide modules or polyproteins (Ott *et al.* 2016). These two approaches allow for a clearer isolation of the protein being unfolded, thereby minimizing the interference from the tethering surfaces and limiting the danger of simultaneous

manipulation of multiple chains. However, in the context of protein aggregation, the presence of such handles or a system composed by multiple repeats is a poor option, because it would introduce new types of intermolecular interactions that may alter the aggregation process. There is therefore the danger that manipulation of small proteins with their natural composition will contain events that result from the pulling of several chains in parallel. This is particularly true in aggregated species due the high proximity between different protein molecules.

It has been shown that the pulling of two polypeptide chains in parallel results in an apparent halving of *Lp* values with respect to the 0.4 nm expected for a single polypeptide chain (Sarkar *et al.* 2007). We therefore used the criterion of accepting a curve for further analysis if under unconstrained fitting of the WLC the fraction of events with $Lp > 0.3$ nm would be greater than that of events with $Lp < 0.3$ nm. A 0.1 nm tolerance in *Lp* with respect to the expected 0.4 nm was introduced to account for the fact that the majority of unfolding events occurred over fairly small length scales (~ 10 nm), and for the impact of pulling geometry over short distances. In both cases, the fitting accuracy can be compromised and the apparent *Lp* deviates from the expected value. Despite the fact that no upper limit for *Lp* was imposed, the curves thus selected for analysis resulted in average and median *Lp* values that are very close to 0.4 nm in both nTTR and aoTTR (Figure 2C). In both cases a frequency distribution with a main peak at 0.4 nm was observed (Figure 2C). For aoTTR the occurrence of force transitions with $Lp< 0.4$ is more pronounced and is likely a result of the more condensed state of the sample. Indeed, they appear to have a greater impact for events that occur closer to the surface in the case of aoTTR, but are typically absent in the case of nTTR (Figure S1). Altogether, the values of *Lp* obtained from fits of the WLC model to the transitions observed fall within those reported in the literature, which typically vary between 0.31 nm for a glycine homopolymer and 0.59 nm for stiffer polypeptides with high ψ dihedral angle potentials (Stirnemann *et al.* 2013).

Contour length of manipulated chains.

Analysis of the contour length of the final event reveals striking differences between the two samples analyzed. It indicates that the manipulated chains in aoTTR are longer than those of nTTR (Figure 4A). Since the TTR monomer is 128 residues long, or 51.2 nm (considering a 0.4 nm length for each residue), we can see that while in the case of nTTR only a fraction of the TTR monomer was manipulated, for aoTTR the manipulated chains are greater than that of a single monomer and likely correspond to the distance of a TTR dimer (Figure 4). The observation in aoTTR of chain lengths that are equivalent to that of a dimer, but not more, is suggestive of a head-to-head and tail-

to-tail orientation of the monomers (Figure 5D). If monomers associated in a head-to-tail arrangement, then the monomer-monomer interface would be replicated at every interface, resulting in a polymeric arrangement and hence much longer chains and apparent contour lengths. In fact, earlier studies suggest that head-to-head dimers may serve as basic building blocks for the assembly of TTR amyloid aggregates that may share the same subunit interface as the native dimer (Serag *et al.* 2001). In that study the authors reported that TTR monomers containing cysteine mutations in the F-strand resulting in cross-linked head-to-head dimers, produced amyloid aggregates with very similar kinetic profile as the wild-type form of the protein. A follow-up study from the same group further suggested extensive rearrangement of the edge strands C and D that exposed residues of strand B which would hence partake a new amyloid TTR interface (Serag *et al.* 2002). More recently, the design of peptides that specifically bind to strands F and H of TTR have been shown to effectively work as amyloid inhibitors by capping those strands and preventing head-to-head association of TTR monomers (Saelices *et al.* 2015). The particular relevance of dimers over other similar low molecular weight aggregates (e.g. trimers, tetramers, pentamers), is not exclusive to TTR and has been reported in a variety of amyloidogenic systems such as peptides Aβ (Lopez del Amo *et al.* 2012) and Sup35 (Zhang *et al.* 2007), as well as proteins, including α-synuclein (Lv *et al.* 2016, Marmolino *et al.* 2016), and β2-microglobulin (Mendoza *et al.* 2010). Thus, it is conceivable that the arrangement of monomers along the aoTTR annuli might result in alternating strongly and weekly interacting monomer-monomer interfaces, with the strong interfaces associated with dimer formation and weak interfaces defining the dimer outer limits. Interestingly, recent X-ray crystallography data of annular oligomers formed by a derivative of the amyloidogenic Aβ17-36 peptide also pointed at the presence of two distinct types of interfaces (Kreutzer *et al.* 2016). Here it is important to note the shape of the frequency distribution of Lc-Max for aoTTR that displays a sharp decline prior to reaching the complete contour length of a dimer (Figure 4A). This is indicative of a discontinuity with precise physical boundaries. This boundary is less clear for nTTR as the full contour length of the TTR monomer is approached (Figure 4A). X-ray crystallographic structures show that for native TTR the monomer-monomer interface forming the native dimer is stabilized by hydrogen-bonding across the F-strand (Figure 1). Our AFM images of nTTR (Figure 2D) suggest that a mixture of both monomers and dimers is likely to be present. Therefore, while for nTTR the chain length of the TTR monomer does not represent an unsurmountable limit for Lc-Max values, this limit appears to be more defined at the level of the dimer for aoTTR. In addition, the high frequency of pullings observed for chains that are up to ~1.8× the length of the TTR monomer (Figure 4A) is also suggestive that the interface might occur at the termini of the monomer sequence. This corroborates findings in previous reports already discussed here, where

the monomer-monomer interface of the amyloidogenic dimer likely involves residues of the edge strands that lie towards the C-terminus of the sequence (Serag *et al.* 2001;2002, Saelices *et al.* 2015). In fact, for aoTTR we observe pullings that on average are 1.41× the monomer contour length (or ~72 nm) which is remarkably close to a structure of two symmetrically oriented TTR monomers overlapping at their F-strands, which would result in a structure 1.46× the size of a monomer (or ~75 nm long). The fact that we observe curves which can be even longer is indicative that residues in the F strand are not the only ones participating in the interface and, as proposed earlier (Saelices *et al.* 2015), additional residues further downstream of the F strand are also involved in forming the internal dimer interface (Figure 5C).

Contour-length of unfolding intermediates.

Pulling on aoTTR revealed a series of unfolding intermediates (Figure 3A). Typically, two intermediates were observed, corresponding to 3 events per force-extension curve (Figure 3B). In fact, we did not observe any curves in aoTTR that passed our selection criterion, and that would contain no intermediates. This is in striking contrast with the nTTR where ~70% of curves showed the unfolding of the manipulated chain in a single step (Figure 3B). The immunoglobulin domain I27 of the sarcomeric protein Titin, which has been extensively used in force spectroscopy experiments (Hoffmann *et al.* 2012), typically unfolds through overcoming a single energy barrier (Fowler *et al.* 2002, Hoffmann *et al.* 2012). Like the TTR monomer, the I27 domain is a β-sheet protein containing eight-strands forming two beta-sheets that stack on in each other to form a β-sandwich fold, and revealing a so called “Greek key” topological motif. Interestingly, molecular dynamic simulations reveal that the I27 dimer, rather than the trimer or the tetramer, is the smallest unit that will spontaneously misfold (Zheng *et al.* 2013). Differences in the extent with which unfolding intermediates are observed in aoTTR in comparison to nTTR are suggestive of considerable folding differences, but also of stabilization of unfolding intermediates of the aoTTR dimer by its neighboring environment. To illustrate this last point, we may take the example of two different classes of α-helical proteins: while membrane-embedded G-protein coupled receptors tend to unfold via the stepwise unravelling of their individual transmembrane α-helices (Zocher *et al.* 2013), soluble α-helical bundles of spectrin unfold in a single event (Law *et al.* 2003). Likewise, mechanical unfolding of β-barrel membrane proteins such as OmpG reveals multiple unfolding intermediates while the water-soluble β-barrel GFP does not (Hensen *et al.* 2013). Thus, the molecular environment in which a protein is found during unfolding has a strong impact in defining the roughness of a protein’s folding energy landscape. This is believed to result from the fact that as proteins unfold in solution, water molecules begin to destabilize its hydrophobic core, thereby

smoothing (and also lowering) the energy profiles leading to the unfolded state (Hensen *et al.* 2013). In a membrane however, the presence of lipid molecules will shield hydrophobic regions from the solvent. As each transmembrane region is loaded and stretched out, the hydrophobic core and hydrophilic lipid headgroups will stabilize the remaining sections of the protein still inserted in the membrane bilayer, thus providing steep energy barriers to the unfolding of intermediates (Hensen *et al.* 2013). Therefore, it is conceivable that the unfolding intermediates observed during pulling of aoTTR derive from the stability provided by contacts between dimers within the annular assembly. It has long been recognized that in the general case of protein aggregation, and of amyloid formation in particular, hydrophobic interactions play a key role in protein condensation. In this regard transthyretin aggregation is no different (Sant'Anna *et al.* 2014). Furthermore, the importance of a yet unknown network of hydrogen-bonding that may be formed across dimers may also be relevant. Previous detailed topographic characterization of aoTTRs indicates that these oligomers assemble to form a stack of two annuli, as suggested by a bimodal distribution of their heights with peaks a ~1 nm for one annulus, and ~2 nm for two annuli (Pires *et al.* 2011). Here, given their average height of 2.45 nm (Figure 2E), annular oligomers appear to predominantly belong to the second population, formed of stacked annuli. Thus, it is conceivable that it was in a context where dimers establish contacts not only along the axis of revolution of the annuli, but also between its two layers, that the unfolding of aoTTR dimers took place (Figure 5C).

Analysis of the average contour length as a function of the ranked order of the unfolding events indicates that transitions appear to be typically separated by ~10 nm with standard deviations in the same range (Figure 4B). Using a curve containing the largest number of events as a reference, and by offsetting several curves by ± 10 nm with respect to the reference curve, we were able to overlay several force spectra that highlight a fairly regular unfolding pattern in aoTTR dimers (Figure 5A). This pattern shows transitions that are separated by ~8 nm, consistent with the frequency distribution of ΔLc values where a predominant peak at ~8 nm is observed (Figure 4C) and closely matching the increment in contour length observed in figure 4B. Such unfolding pattern closely replicated in different pulling experiments underscores the highly organized structure of the system being probed. It suggests that the underlying organization and structure of a given molecule can be observed in a recurrent fashion, in different molecules. The ΔLc distribution also suggests the presence of a fundamental mode at ~4 nm, and additional modes at ~12 and ~18 nm. Considering the contour length of the secondary structure elements in TTR, these values are compatible with the sequential unfolding of β-strands (Figure 5B). Since the exact structure of TTR within amyloid aggregates is currently unknown, it is at this stage speculative to infer whether these transitions

represent the peeling of individual large β-strands or blocks of smaller β-strands such as a hairpin of two consecutive β-strands. However, several reports have highlighted that the structure of TTR within these aggregates might share many similarities with the native conformation of the TTR monomer. The native TTR monomer comprises a series of eight β-strands and one α-helix joined by 8 interconnecting segments and two terminal regions (Figure 5B). On average, each of these regions has a length of 2.7 nm which would mean that an unfolding step with a length ~8 nm would corresponds to the extension of 3 of these sections (8.1 nm). It could, for example, correspond to the stretching and unfolding of β-hairpin structure. Regardless, an extensive dimer-dimer interface will have to exist along the outer surface of at least one of the β-sheets promoting the stabilization of its β-strands. This type of dimer-dimer interface will likely be very different from that found in the tetrameric arrangement of the two native TTR dimers which relies on very weak interactions that need to be stabilized in order to mitigate conversion of TTR into its amyloidogenic form.

Unfolding force of intermediates.

Manipulation of aoTTR resulted in the emergence of intermediates whose mechanical transitions occurred at higher force values than those observed in nTTR (Figure 4D). This difference could be interpreted as a result of the fact that amyloid oligomers typically attain a more stable state than the native protein from which they are derived (De Simone *et al.* 2008, Chang *et al.* 2009, Blinov *et al.* 2010, Berhanu *et al.* 2011, Li *et al.* 2012, Kahler *et al.* 2013, Porrini *et al.* 2013, Berhanu *et al.* 2014, Socher *et al.* 2014). However, such interpretation should be viewed with some caution. On one hand, we are comparing the unfolding forces of intermediates which emerged more rarely in the case of nTTR. For nTTR, most of the force values were discarded from the analysis as these correspond to curves that contained no intermediates, and the force of those transitions is ultimately the result of the tip-sample interaction. On the other hand, mechanical strength of proteins may not necessarily correlate with their thermodynamic stability (Oberhauser *et al.* 2002). It is viewed that pre-fibrillary precursors sample distinct conformations as they travel along a rough energy landscape towards more stable conformations (Gershenson *et al.* 2014). However, along this process they may become kinetically trapped (Hagan *et al.* 2011) in conformations that result in what are called “off-pathway” oligomers (Bellesia *et al.* 2009, Ma *et al.* 2010, Uversky 2010), which may or may not be necessarily more stable than the native conformation (Brummitt *et al.* 2012). Little is known about the stability of annular oligomers and of the dimers found within them. Although they may have crossed an energy barrier that may lead to a more stable arrangement, at this stage the aoTTR dimer may still not represent a more stable conformation when compared to nTTR. An increase in force may be explained by a variety of reasons which with our approach may

be difficult to scrutinize. For example, as highlighted in the previous paragraphs, manipulation of aoTTR dimer occurred in a context where intermolecular interactions between neighboring dimers, and differences in buffer composition can play an important role. Since AFM imaging suggests that nTTR was mostly present in the monomeric form (Figure 2D and 2E), differences in the molecular context of the manipulated chains limit our ability to compare force values. As discussed earlier, the importance of molecular context can be relevant in the definition of the roughness of the energy landscape. In addition, the pulling geometry can have an impact on force as shown earlier for the unfolding of a β-sheet protein (Brockwell *et al.* 2003). Given the annular arrangement of oligomers, it is conceivable that they are organized in a preferential orientation with respect to the pulling axis, rather than randomly distributed which we anticipate to be more likely in the case of nTTR molecules. If so, a preferential orientation with respect to the pulling direction may emphasize one particular unfolding trajectory for which higher forces would be required, while for the case of nTTR these trajectories would be more widely sampled and thus averaged out.

CONCLUSION

We demonstrate using single-molecule force spectroscopy, that native TTR and annular oligomers exhibit distinct unfolding patterns. While nTTR tends to retain a monomeric structure and unfolds in one step, aoTTR unfolds via a series of intermediate structures across a length range equivalent to the contour length of a concatenated TTR dimer. These intermediate structures display a contour-length increment of ~ 8 nm which corresponds to a section of protein chain likely stabilized by intermolecular contacts established by aoTTR dimers within the annular assembly. Monomers arranged in a head-to-head orientation may form an interface that shares some structural similarities with the native dimer. However, when compared with the native tetrameric molecule, dimers in aoTTR are likely to interact with other dimers in a very different way, notably through extensive contacts along their β-strands.

In general, we have shown that through careful selection of force curves using persistence length as a criterion, we are able to select data which can be interpreted and rationalized in agreement with data available for the aggregation pathway of TTR. Since this approach requires no handles, it may open the door to the analysis of other systems which, like ours, may become distorted when analyzed in tandem repeats, or in the presence of molecular handles. In addition, transient structures which may be too dynamic or heterogeneous to be captured by higher resolution methods may, in a similar way, be probed and understood with greater structural detail.

ACKNOWLEDGEMENTS

This work was supported by grants from the Hungarian Science Foundation (OTKA K109480) and the National Research, Development and Innovation Office under the contract **VKSZ_14-1-2015-052**. The research leading to these results has received funding from the European Union's Seventh Framework Program (FP7/2007-2013) under grant agreement n° HEALTH-F2-2011-278850 (INMiND).

ABREVIATIONS

AFM, Atomic Force Microscopy; PBS, phosphate buffer saline; SMFS, single molecule force spectroscopy; TTR, Transthyretin; nTTR, Native transthyretin; aoTTR, Transthyretin amyloid annular oligomers; WT, wild type.

REFERENCES

Almeida, MR, Damas, AM, Lans, MC, Brouwer, A, Saraiva, MJ. 1997. Thyroxine binding to transthyretin Met 119. Comparative studies of different heterozygotic carriers and structural analysis. *Endocrine* **6**(3): 309-315. DOI: 10.1007/BF02820508.

Alshehri, B, D'Souza, DG, Lee, JY, Petratos, S, Richardson, SJ. 2015. The diversity of mechanisms influenced by transthyretin in neurobiology: development, disease and endocrine disruption. *J Neuroendocrinol* **27**(5): 303-323. DOI: 10.1111/jne.12271.

Annamalai, K, Guhrs, KH, Koehler, R, Schmidt, M, Michel, H, Loos, C, Gaffney, PM, Sigurdson, CJ, Hegenbart, U, Schonland, S, Fandrich, M. 2016. Polymorphism of Amyloid Fibrils In Vivo. *Angew Chem Int Ed Engl* DOI: 10.1002/anie.201511524.

Bellesia, G, Shea, JE. 2009. Diversity of kinetic pathways in amyloid fibril formation. *J Chem Phys* **131**(11): 111102. DOI: 10.1063/1.3216103.

Berhanu, WM, Hansmann, UH. 2014. Stability of amyloid oligomers. *Adv Protein Chem Struct Biol* **96**: 113-141. DOI: 10.1016/bs.apcsb.2014.06.006.

Berhanu, WM, Masunov, AE. 2011. Can molecular dynamics simulations assist in design of specific inhibitors and imaging agents of amyloid aggregation? Structure, stability and free energy predictions for amyloid oligomers of VQIVYK, MVGGVV and LYQLEN. *J Mol Model* **17**(10): 2423-2442. DOI: 10.1007/s00894-010-0912-4.

Blinov, N, Dorosh, L, Wishart, D, Kovalenko, A. 2010. Association thermodynamics and conformational stability of beta-sheet amyloid beta(17-42) oligomers: effects of E22Q (Dutch) mutation and charge neutralization. *Biophys J* **98**(2): 282-296. DOI: 10.1016/j.bpj.2009.09.062.

Brockwell, DJ, Paci, E, Zinober, RC, Beddard, GS, Olmsted, PD, Smith, DA, Perham, RN, Radford, SE. 2003. Pulling geometry defines the mechanical resistance of a beta-sheet protein. *Nat Struct Biol* **10**(9): 731-737. DOI: 10.1038/nsb968.

Brummitt, RK, Andrews, JM, Jordan, JL, Fernandez, EJ, Roberts, CJ. 2012. Thermodynamics of amyloid dissociation provide insights into aggregate stability regimes. *Biophys Chem* **168-169**: 10-18. DOI: 10.1016/j.bpc.2012.06.001.

Capone, R, Quiroz, FG, Prangkio, P, Saluja, I, Sauer, AM, Bautista, MR, Turner, RS, Yang, J, Mayer, M. 2009. Amyloid-beta-Induced Ion Flux in Artificial Lipid Bilayers and Neuronal Cells: Resolving a Controversy. *Neurotoxicity Research* **16**(1): 1-13.

Cardoso, I, Goldsbury, CS, Muller, SA, Olivieri, V, Wirtz, S, Damas, AM, Aebi, U, Saraiva, MJ. 2002. Transthyretin fibrillogenesis entails the assembly of monomers: a molecular model for in vitro assembled transthyretin amyloid-like fibrils. *J Mol Biol* **317**(5): 683-695. DOI: 10.1006/jmbi.2002.5441.

Cecchi, C, Stefani, M. 2013. The amyloid-cell membrane system. The interplay between the biophysical features of oligomers/fibrils and cell membrane defines amyloid toxicity. *Biophysical Chemistry* **182**: 30-43.
Cecconi, C, Shank, EA, Marqusee, S, Bustamante, C. 2011. DNA molecular handles for single-molecule protein-folding studies by optical tweezers. *Methods Mol Biol* **749**: 255-271. DOI: 10.1007/978-1-61779-142-0_18.
Chang, LK, Zhao, JH, Liu, HL, Liu, KT, Chen, JT, Tsai, WB, Ho, Y. 2009. Molecular dynamics simulations to investigate the structural stability and aggregation behavior of the GGVVIA oligomers derived from amyloid beta peptide. *J Biomol Struct Dyn* **26**(6): 731-740. DOI: 10.1080/07391102.2009.10507285.
Damas, AM, Saraiva, MJ. 2000. Review: TTR amyloidosis-structural features leading to protein aggregation and their implications on therapeutic strategies. *J Struct Biol* **130**(2-3): 290-299. DOI: 10.1006/jsbi.2000.4273.
De Simone, A, Esposito, L, Pedone, C, Vitagliano, L. 2008. Insights into stability and toxicity of amyloid-like oligomers by replica exchange molecular dynamics analyses. *Biophys J* **95**(4): 1965-1973. DOI: 10.1529/biophysj.108.129213.
Diomede, L, Di Fede, G, Romeo, M, Bagnati, R, Ghidoni, R, Fiordaliso, F, Salio, M, Rossi, A, Catania, M, Paterlini, A, Benussi, L, Bastone, A, Stravalaci, M, Gobbi, M, Tagliavini, F, Salmona, M. 2014. Expression of A2V-mutated Abeta in Caenorhabditis elegans results in oligomer formation and toxicity. *Neurobiol Dis* **62**: 521-532. DOI: 10.1016/j.nbd.2013.10.024.
Faria, TQ, Almeida, ZL, Cruz, PF, Jesus, CS, Castanheira, P, Brito, RM. 2015. A look into amyloid formation by transthyretin: aggregation pathway and a novel kinetic model. *Phys Chem Chem Phys* **17**(11): 7255-7263. DOI: 10.1039/c4cp04549a.
Fowler, SB, Best, RB, Toca Herrera, JL, Rutherford, TJ, Steward, A, Paci, E, Karplus, M, Clarke, J. 2002. Mechanical unfolding of a titin Ig domain: structure of unfolding intermediate revealed by combining AFM, molecular dynamics simulations, NMR and protein engineering. *J Mol Biol* **322**(4): 841-849.
Gershenson, A, Gierasch, LM, Pastore, A, Radford, SE. 2014. Energy landscapes of functional proteins are inherently risky. *Nat Chem Biol* **10**(11): 884-891. DOI: 10.1038/nchembio.1670.
Groenning, M, Campos, RI, Hirschberg, D, Hammarstrom, P, Vestergaard, B. 2015. Considerably Unfolded Transthyretin Monomers Preceed and Exchange with Dynamically Structured Amyloid Protofibrils. *Sci Rep* **5**: 11443. DOI: 10.1038/srep11443.
Hagan, MF, Elrad, OM, Jack, RL. 2011. Mechanisms of kinetic trapping in self-assembly and phase transformation. *J Chem Phys* **135**(10): 104115. DOI: 10.1063/1.3635775.
Harte, NP, Klyubin, I, McCarthy, EK, Min, S, Garrahy, SA, Xie, Y, Davey, GP, Boland, JJ, Rowan, MJ, Mok, KH. 2015. Amyloid Oligomers and Mature Fibrils Prepared from an Innocuous Protein Cause Diverging Cellular Death Mechanisms. *J Biol Chem* **290**(47): 28343-28352. DOI: 10.1074/jbc.M115.676072.
Hensen, U, Muller, DJ. 2013. Mechanistic explanation of different unfolding behaviors observed for transmembrane and soluble beta-barrel proteins. *Structure* **21**(8): 1317-1324. DOI: 10.1016/j.str.2013.06.001.
Hoffmann, T, Dougan, L. 2012. Single molecule force spectroscopy using polyproteins. *Chemical Society Reviews* **41**(14): 4781-4796.
Hutter, JL, Bechhoefer, J. 1993. Calibration of Atomic-Force Microscope Tips. *Review of Scientific Instruments* **64**(7): 1868-1873.
Johnson, SM, Wiseman, RL, Sekijima, Y, Green, NS, Adamski-Werner, SL, Kelly, JW. 2005. Native state kinetic stabilization as a strategy to ameliorate protein misfolding diseases: A focus on the transthyretin amyloidoses. *Accounts of Chemical Research* **38**(12): 911-921.

Kahler, A, Sticht, H, Horn, AH. 2013. Conformational stability of fibrillar amyloid-beta oligomers via protofilament pair formation - a systematic computational study. *PLoS One* **8**(7): e70521. DOI: 10.1371/journal.pone.0070521.
Kreutzer, AG, Hamza, IL, Spencer, RK, Nowick, JS. 2016. X-ray Crystallographic Structures of a Trimer, Dodecamer, and Annular Pore Formed by an Abeta17-36 beta-Hairpin. *J Am Chem Soc* DOI: 10.1021/jacs.6b01332.
Lai, Z, Colon, W, Kelly, JW. 1996. The acid-mediated denaturation pathway of transthyretin yields a conformational intermediate that can self-assemble into amyloid. *Biochemistry* **35**(20): 6470-6482. DOI: 10.1021/bi952501g.
Lasagna-Reeves, CA, Sengupta, U, Castillo-Carranza, D, Gerson, JE, Guerrero-Munoz, M, Troncoso, JC, Jackson, GR, Kayed, R. 2014. The formation of tau pore-like structures is prevalent and cell specific: possible implications for the disease phenotypes. *Acta Neuropathol Commun* **2**: 56. DOI: 10.1186/2051-5960-2-56.
Law, R, Carl, P, Harper, S, Dalhaimer, P, Speicher, DW, Discher, DE. 2003. Cooperativity in forced unfolding of tandem spectrin repeats. *Biophys J* **84**(1): 533-544. DOI: 10.1016/S0006-3495(03)74872-3.
Li, Y, Ji, C, Xu, W, Zhang, JZ. 2012. Dynamical stability and assembly cooperativity of beta-sheet amyloid oligomers--effect of polarization. *J Phys Chem B* **116**(45): 13368-13373. DOI: 10.1021/jp3086599.
Lopez del Amo, JM, Schmidt, M, Fink, U, Dasari, M, Fandrich, M, Reif, B. 2012. An asymmetric dimer as the basic subunit in Alzheimer's disease amyloid beta fibrils. *Angew Chem Int Ed Engl* **51**(25): 6136-6139. DOI: 10.1002/anie.201200965.
Lv, Z, Krasnoslobodtsev, AV, Zhang, Y, Ysselstein, D, Rochet, JC, Blanchard, SC, Lyubchenko, YL. 2016. Effect of acidic pH on the stability of alpha-Synuclein dimers. *Biopolymers* DOI: 10.1002/bip.22874.
Ma, B, Nussinov, R. 2010. Polymorphic C-terminal beta-sheet interactions determine the formation of fibril or amyloid beta-derived diffusible ligand-like globulomer for the Alzheimer Abeta42 dodecamer. *J Biol Chem* **285**(47): 37102-37110. DOI: 10.1074/jbc.M110.133488.
Maleszewski, JJ. 2015. Cardiac amyloidosis: pathology, nomenclature, and typing. *Cardiovasc Pathol* **24**(6): 343-350. DOI: 10.1016/j.carpath.2015.07.008.
Marmolino, D, Foerch, P, Atienzar, FA, Staelens, L, Michel, A, Scheller, D. 2016. Alpha synuclein dimers and oligomers are increased in overexpressing conditions in vitro and in vivo. *Mol Cell Neurosci* **71**: 92-101. DOI: 10.1016/j.mcn.2015.12.012.
Mendoza, VL, Antwi, K, Baron-Rodriguez, MA, Blanco, C, Vachet, RW. 2010. Structure of the preamyloid dimer of beta-2-microglobulin from covalent labeling and mass spectrometry. *Biochemistry* **49**(7): 1522-1532. DOI: 10.1021/bi901748h.
Mirzabekov, TA, Lin, MC, Kagan, BL. 1996. Pore formation by the cytotoxic islet amyloid peptide amylin. *Journal of Biological Chemistry* **271**(4): 1988-1992.
Mulaj, M, Foley, J, Muschol, M. 2014. Amyloid oligomers and protofibrils, but not filaments, self-replicate from native lysozyme. *J Am Chem Soc* **136**(25): 8947-8956. DOI: 10.1021/ja502529m.
Muller, DJ, Engel, A. 2007. Atomic force microscopy and spectroscopy of native membrane proteins. *Nat Protoc* **2**(9): 2191-2197. DOI: 10.1038/nprot.2007.309.
Nagasaka, T. 2012. Familial amyloidotic polyneuropathy and transthyretin. *Subcell Biochem* **65**: 565-607. DOI: 10.1007/978-94-007-5416-4_21.
Naiki, H, Okoshi, T, Ozawa, D, Yamaguchi, I, Hasegawa, K. 2016. Molecular pathogenesis of human amyloidosis: Lessons from beta -microglobulin-related amyloidosis. *Pathol Int* DOI: 10.1111/pin.12394.
Nakagawa, M, Sekijima, Y, Yazaki, M, Tojo, K, Yoshinaga, T, Doden, T, Koyama, J, Yanagisawa, S, Ikeda, S. 2016. Carpal tunnel syndrome: a common initial symptom of systemic wild-type ATTR (ATTRwt) amyloidosis. *Amyloid* **23**(1): 58-63. DOI: 10.3109/13506129.2015.1135792.

Nixon, RA, Cataldo, AM. 2006. Lysosomal system pathways: genes to neurodegeneration in Alzheimer's disease. *J Alzheimers Dis* **9**(3 Suppl): 277-289.
Oberhauser, AF, Badilla-Fernandez, C, Carrion-Vazquez, M, Fernandez, JM. 2002. The mechanical hierarchies of fibronectin observed with single-molecule AFM. *J Mol Biol* **319**(2): 433-447. DOI: 10.1016/S0022-2836(02)00306-6.
Ott, W, Jobst, MA, Schoeler, C, Gaub, HE, Nash, MA. 2016. Single-molecule force spectroscopy on polyproteins and receptor-ligand complexes: The current toolbox. *J Struct Biol* DOI: 10.1016/j.jsb.2016.02.011.
Pires, RH, Karsai, A, Saraiva, MJ, Damas, AM, Kellermayer, MS. 2012. Distinct annular oligomers captured along the assembly and disassembly pathways of transthyretin amyloid protofibrils. *PLoS One* **7**(9): e44992. DOI: 10.1371/journal.pone.0044992.
Pires, RH, Saraiva, MJ, Damas, AM, Kellermayer, MS. 2011. Structure and assembly-disassembly properties of wild-type transthyretin amyloid protofibrils observed with atomic force microscopy. *J Mol Recognit* **24**(3): 467-476. DOI: 10.1002/jmr.1112.
Porrini, M, Zachariae, U, Barran, PE, MacPhee, CE. 2013. Effect of Protonation State on the Stability of Amyloid Oligomers Assembled from TTR(105-115). *J Phys Chem Lett* **4**(8): 1233-1238. DOI: 10.1021/jz400372u.
Quintas, A, Saraiva, MJ, Brito, RM. 1997. The amyloidogenic potential of transthyretin variants correlates with their tendency to aggregate in solution. *FEBS Lett* **418**(3): 297-300.
Quist, A, Doudevski, I, Lin, H, Azimova, R, Ng, D, Frangione, B, Kagan, B, Ghiso, J, Lal, R. 2005. Amyloid ion channels: a common structural link for protein-misfolding disease. *Proc Natl Acad Sci U S A* **102**(30): 10427-10432. DOI: 10.1073/pnas.0502066102.
Robbins, J. 2002. Transthyretin from discovery to now. *Clin Chem Lab Med* **40**(12): 1183-1190. DOI: 10.1515/CCLM.2002.208.
Saelices, L, Johnson, LM, Liang, WY, Sawaya, MR, Cascio, D, Ruchala, P, Whitelegge, J, Jiang, L, Riek, R, Eisenberg, DS. 2015. Uncovering the Mechanism of Aggregation of Human Transthyretin. *J Biol Chem* **290**(48): 28932-28943. DOI: 10.1074/jbc.M115.659912.
Sant'Anna, R, Braga, C, Varejao, N, Pimenta, KM, Grana-Montes, R, Alves, A, Cortines, J, Cordeiro, Y, Ventura, S, Foguel, D. 2014. The importance of a gatekeeper residue on the aggregation of transthyretin: implications for transthyretin-related amyloidoses. *J Biol Chem* **289**(41): 28324-28337. DOI: 10.1074/jbc.M114.563981.
Sarkar, A, Caamano, S, Fernandez, JM. 2007. The mechanical fingerprint of a parallel polyprotein dimer. *Biophys J* **92**(4): L36-38. DOI: 10.1529/biophysj.106.097741.
Sbrana, F, Bongini, L, Cappugi, G, Fanelli, D, Guarino, A, Pazzagli, L, Scala, A, Vassalli, M, Zoppi, C, Tiribilli, B. 2007. Atomic force microscopy images suggest aggregation mechanism in cerato-platanin. *Eur Biophys J* **36**(7): 727-732. DOI: 10.1007/s00249-007-0159-x.
Serag, AA, Altenbach, C, Gingery, M, Hubbell, WL, Yeates, TO. 2001. Identification of a subunit interface in transthyretin amyloid fibrils: evidence for self-assembly from oligomeric building blocks. *Biochemistry* **40**(31): 9089-9096.
Serag, AA, Altenbach, C, Gingery, M, Hubbell, WL, Yeates, TO. 2002. Arrangement of subunits and ordering of beta-strands in an amyloid sheet. *Nat Struct Biol* **9**(10): 734-739. DOI: 10.1038/nsb838.
Socher, E, Sticht, H, Horn, AH. 2014. The conformational stability of nonfibrillar amyloid-beta peptide oligomers critically depends on the C-terminal peptide length. *ACS Chem Neurosci* **5**(3): 161-167. DOI: 10.1021/cn400208r.
Stirnemann, G, Giganti, D, Fernandez, JM, Berne, BJ. 2013. Elasticity, structure, and relaxation of extended proteins under force. *Proc Natl Acad Sci U S A* **110**(10): 3847-3852. DOI: 10.1073/pnas.1300596110.
Uversky, VN. 2010. Mysterious oligomerization of the amyloidogenic proteins. *FEBS J* **277**(14): 2940-2953. DOI: 10.1111/j.1742-4658.2010.07721.x.

Wang, H, Bash, R, Yodh, JG, Hager, GL, Lohr, D, Lindsay, SM. 2002. Glutaraldehyde modified mica: a new surface for atomic force microscopy of chromatin. *Biophys J* **83**(6): 3619-3625. DOI: 10.1016/S0006-3495(02)75362-9.
Wechalekar, AD, Gillmore, JD, Hawkins, PN. 2015. Systemic amyloidosis. *Lancet* DOI: 10.1016/S0140-6736(15)01274-X.
Yagi, H, Abe, Y, Takayanagi, N, Goto, Y. 2014. Elongation of amyloid fibrils through lateral binding of monomers revealed by total internal reflection fluorescence microscopy. *Biochim Biophys Acta* **1844**(10): 1881-1888. DOI: 10.1016/j.bbapap.2014.06.014.
Zhang, Z, Chen, H, Bai, H, Lai, L. 2007. Molecular dynamics simulations on the oligomer-formation process of the GNNQQNY peptide from yeast prion protein Sup35. *Biophys J* **93**(5): 1484-1492. DOI: 10.1529/biophysj.106.100537.
Zheng, W, Schafer, NP, Wolynes, PG. 2013. Free energy landscapes for initiation and branching of protein aggregation. *Proc Natl Acad Sci U S A* **110**(51): 20515-20520. DOI: 10.1073/pnas.1320483110.
Zocher, M, Bippes, CA, Zhang, C, Muller, DJ. 2013. Single-molecule force spectroscopy of G-protein-coupled receptors. *Chem Soc Rev* **42**(19): 7801-7815. DOI: 10.1039/c3cs60085h.

FIGURES

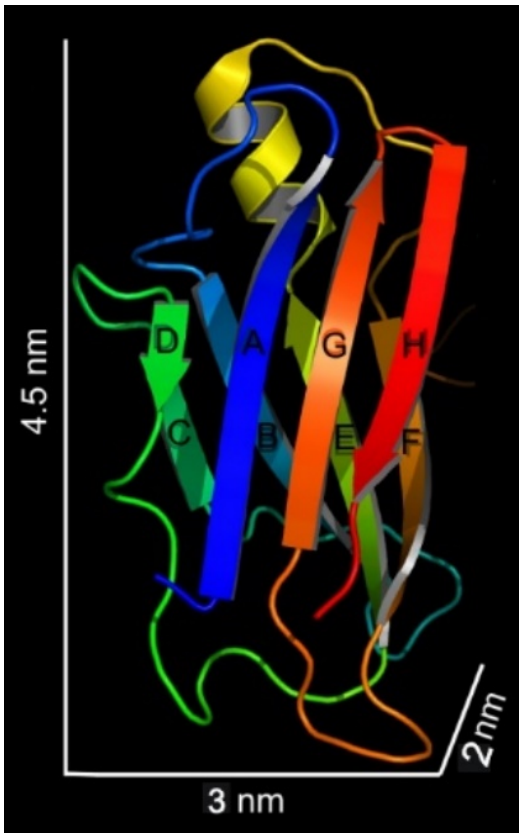

Figure 1: 3D structure of TTR monomer (PDB entry: 2PAB) shows a beta-sandwich conformation by assembly of eight β-strands (A – F) into two β-sheets: DAGH and CBEF.

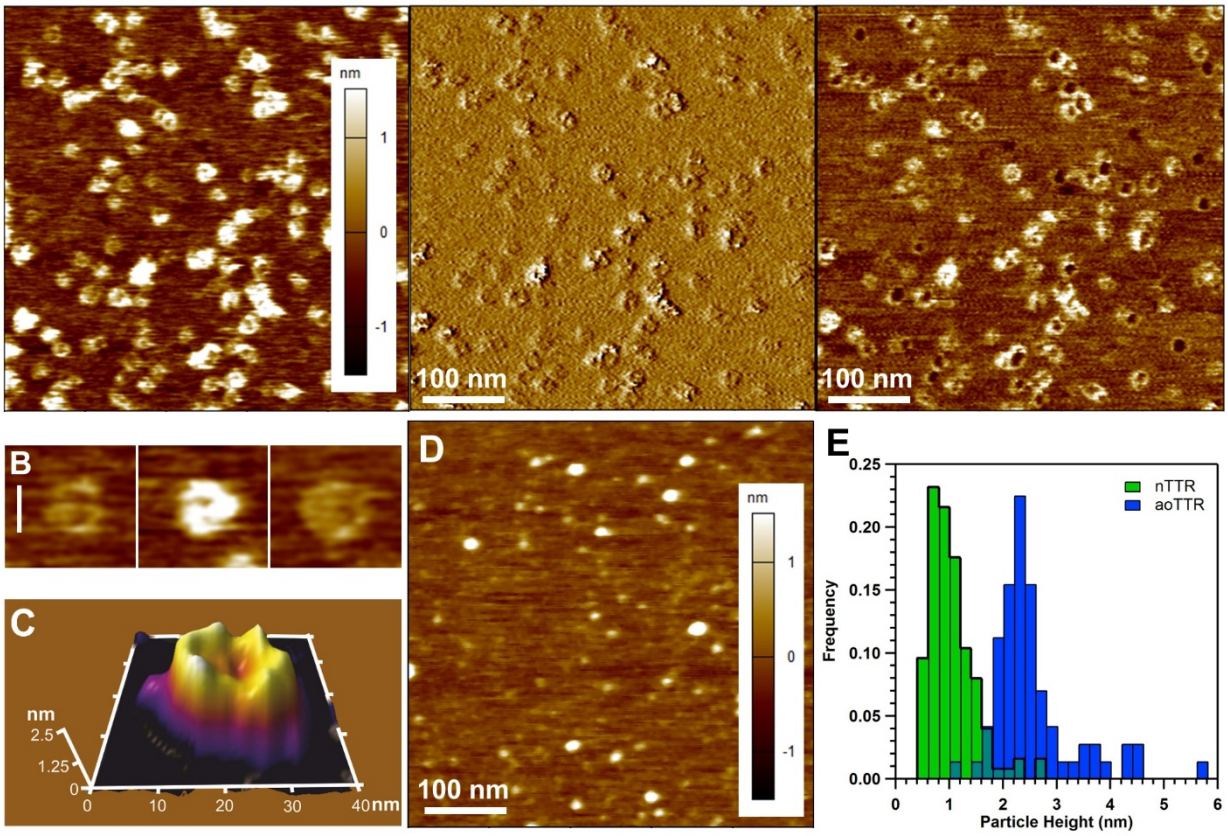

Figure 2: AFM imaging in liquid. (A) Annular oligomers detected by three different contrast modalities: height (left), amplitude (center) and phase (right). (B) Three selected oligomers evidence circular perimeter and a hollow core. Scale bar is 15 nm and applies to all three panels. (C) 3D rendition of the topological map emphasizes annular configuration of oligomers. (D) Images of native TTR dispersed in PBS buffer. (E) Histogram of particle heights. nTTR and aoTTR refer to the native and annular oligomeric forms of TTR.

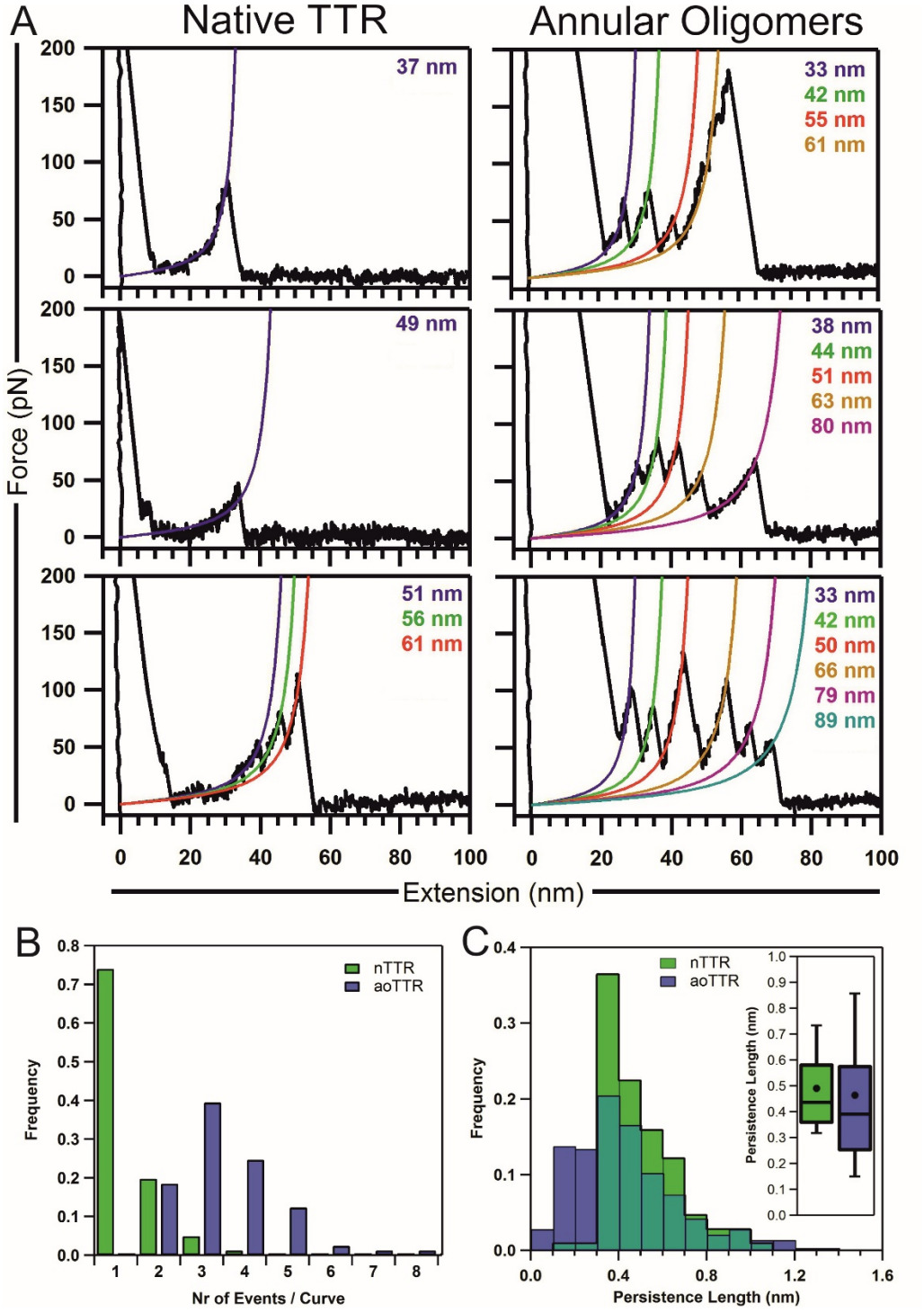

Figure 3: Force spectroscopy data. (A) Comparison of force curves obtained for the native and the amyloid annular oligomeric form of TTR highlights differences with respect to the frequency of force transitions and total length of the manipulated chains. Colored lines are WLC fits with *Lp* = 0.4 nm, and the resulting *Lc* values are indicated on the right. (B) nTTR typically unfolded in a single step, with one event detected per curve, whereas aoTTR curves displayed multiple force peaks. (C) Distribution of persistence lengths using unconstrained WLC fits places the typical *Lp*

for both samples in the neighborhood of 0.4 nm. In the box plots, error bars represent 10-90% range; central line and dot correspond to median and mean, respectively.

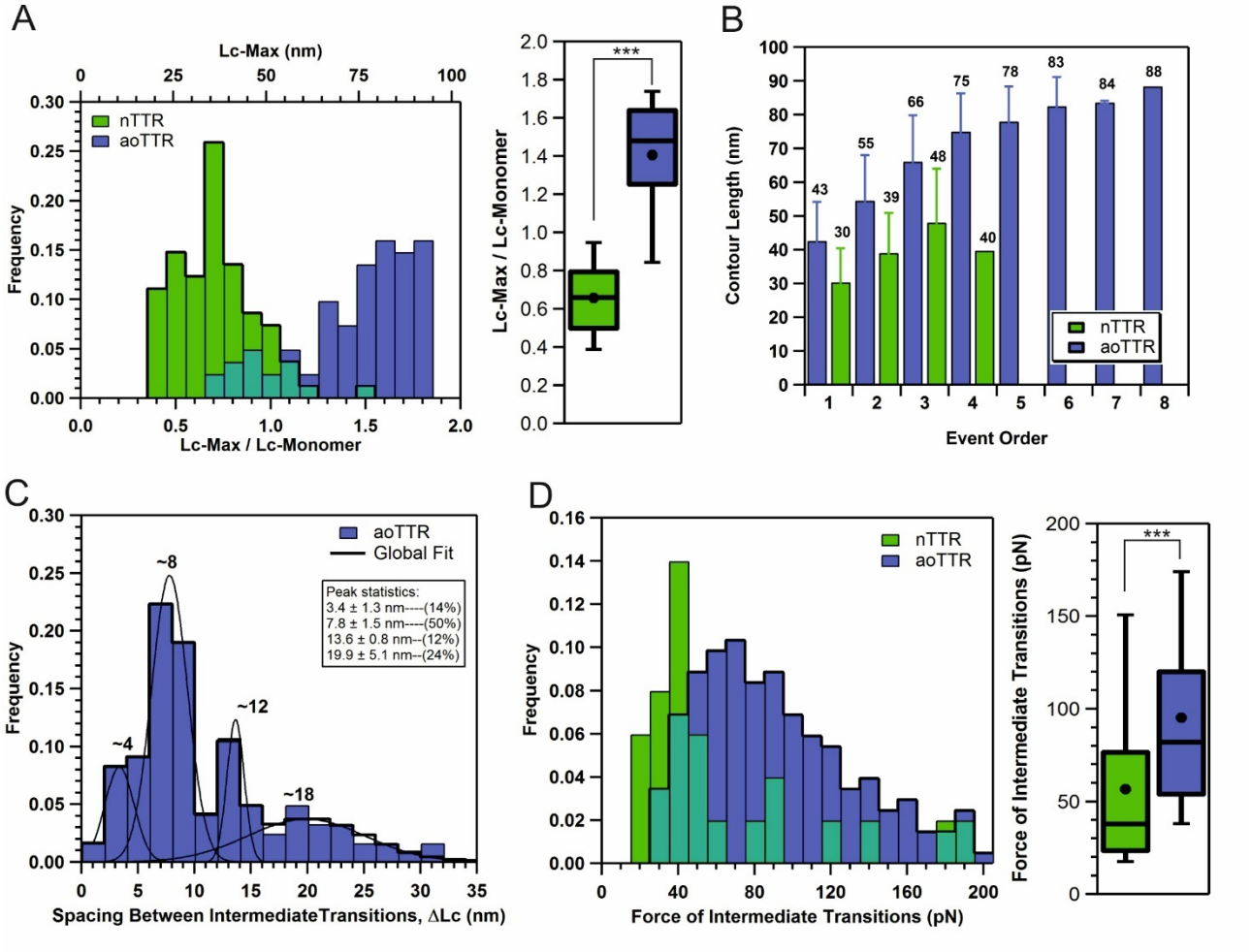

Figure 4: Analysis of contour length and force values. (A) Evaluation of the maximal contour length (Lc-Max) of the manipulated chains shown in distance units (histogram, top axis) and as a fraction of the contour length of the TTR monomer (histogram, bottom axis & box-plot). (B) Average contour length as a function of ranked order of unfolding events within a force spectrum shows that increments of ~10 nm are common. Numbers above bars are the average Lc. The last values of both series are single measurements and therefore contain no error bars. Error bars represent standard deviation. Sample size is 108 for nTTR and 283 aoTTR (C) Histogram of the spacing between consecutive transitions (ΔLc) shows multiples of 4 up to 12 nm, and an additional peak at 18 nm (D) Histogram and box-plot comparison of the force registered for unfolding intermediates. The force of the last event (tip-sample detachment) was discarded from this analysis. In the box plots, error bars represent 10-90% range; central line and dot correspond to median and mean, respectively. Statistical significance at $p<0.001$ is denoted by ***

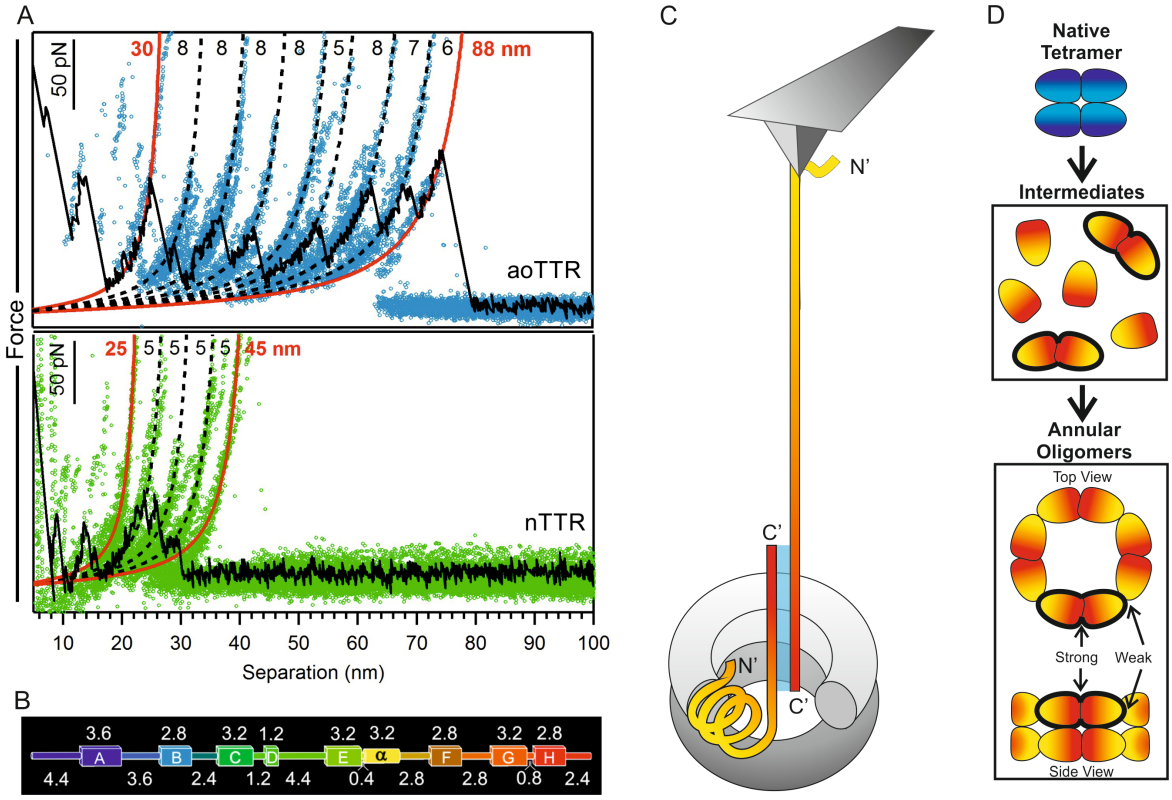

Figure 5: Mechanical unfolding and secondary structure of TTR. (A) Overlay of different curves from the manipulation of aoTTR (above) and nTTR (below). (B) Secondary structure of TTR (PDB entry 2PAB) measured in nanometers (numbers) and where letters (A – H) indicate β-strands and α represents the sole α-helix; colors are as represented in Figure 1. (C) Schematic representation of the pulling of a dimer from aoTTR where dimerization is likely to occur through participation of residues towards the C' terminus. The double-stack arrangement of aoTTR likely contributes to stabilize unfolding intermediates. (D) Diagram of the assembly of annular oligomers with monomers oriented in a head-to-head and tail-to-tail configuration forming strong and weakly interacting interfaces.

SUPPLEMENTARY INFORMATION

Table S1: Summary of relevant statistics

Property	Units	Sample	n	Average	St. Dev.	S.E.M.	Median	p-value
Particle Height	nm	nTTR	125	1.03	0.52	0.05	0.9	<0.001
		aoTTR	71	2.47	0.78	0.09	2.3	
Persistence Length	nm	nTTR	107	0.491	0.171	0.017	0.436	N/A
		aoTTR	283	0.464	0.325	0.019	0.391	
ΔLc between intermediates	nm	aoTTR	121	11.0	6.7	0.6	8.7	N/A
Lc-Max/Lc-Monomer	-	nTTR	81	0.66	0.21	0.02	0.66	<0.001
		aoTTR	81	1.41	0.31	0.03	1.48	
Force of Intermediate Transitions	pN	nTTR	25	57	48	10	38	<0.001
		aoTTR	203	95	55	4	82	

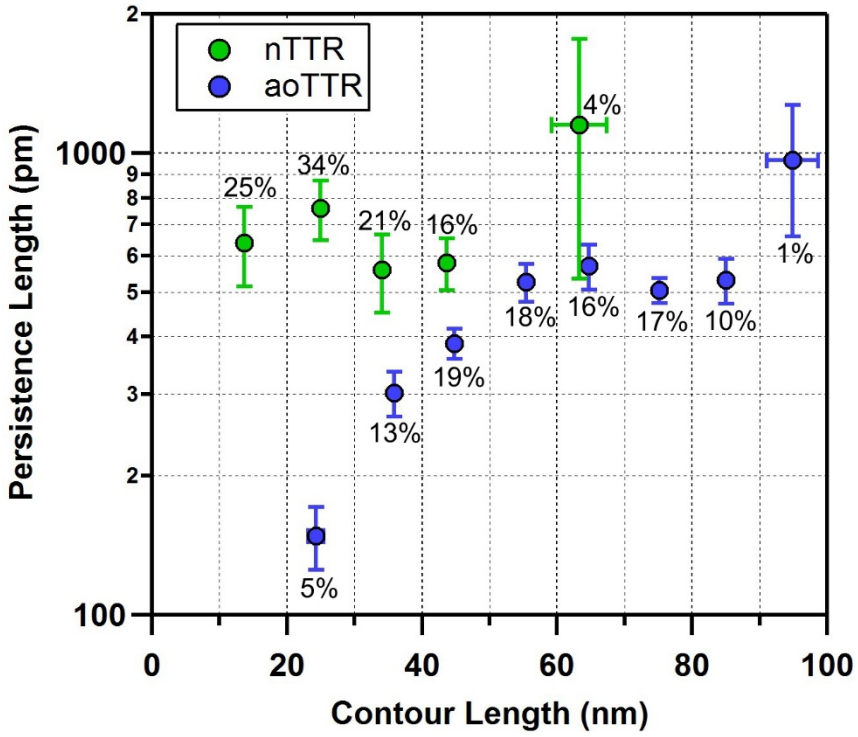

Figure S1: Relationship between contour length (*Lc*) and persistence length (*Lp*) in force transitions registered in the selected curves.

For each event, *Lc* values obtained by fitting the WLC model constrained with *Lp* = 0.4 nm were correlated with the *Lp* obtained from an unconstrained fit of the WLC model. Values were binned in 10 nm intervals of *Lc*, and the average *Lc* plotted against the corresponding average *Lp*. The frequency of events found within each bin with respect to the total number of events is expressed as percentages next to each data point.

Unlike nTTR, oligomers show a tendency for low apparent *Lp* values at low contour lengths, particularly for events taken to have an *Lc* of 20-30 nm. This suggests that within a trace containing multiple force transitions, those occurring in the *Lc* region of 20-30 nm are more likely to reflect pulling of multiple chains. However, these events represent only 5% of all the analyzed force transitions and therefore, their impact on the interpretation of the selected force curves is considered negligible.

Graphical Table of Contents

Transient oligomeric amyloid assemblies remain a challenge for molecular structural studies. Here we show by AFM force spectroscopy that misfolded dimers constitute a key arrangement for the assembly of transthyretin amyloid annular oligomers.

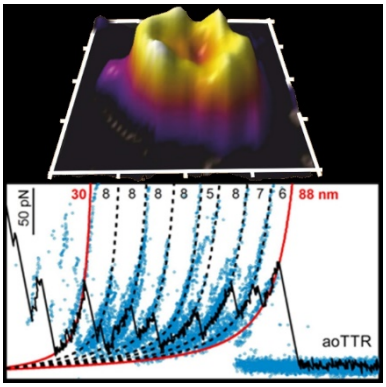

Force Spectroscopy Reveals the Presence of Structurally Modified Dimers in Transthyretin Amyloid Annular Oligomers.

Ricardo H. Pires, Maria J. Saraiva, Ana M. Damas, and Miklós S. Z. Kellermayer